

## RESEARCH ARTICLE

# OPTIMIZATION AND EXPERIMENTAL EVALUATION OF BIO-HYDRAULIC FLUID FROM SPENT PALM KERNEL OIL WITH GRAPHITE, EGGSHELL, AND SNAIL SHELL FRICTION MODIFIERS

Ifediorah E.I.\*, Ezeugo J.O.

Department of Chemical Engineering, Chukwuemeka Odumegwu Ojukwu University, P.M.B. 6059. Anambra state, Nigeria  
 \*Corresponding Author Email: [Ezekielifediorah@gmail.com](mailto:Ezekielifediorah@gmail.com)

This is an open access journal distributed under the Creative Commons Attribution License CC BY 4.0, which permits unrestricted use, distribution, and reproduction in any medium, provided the original work is properly cited.

## ARTICLE DETAILS

## Article History:

Received 7 April 2025  
 Revised 5 May 2025  
 Accepted 10 May 2025  
 Available online 18 June 2025

## ABSTRACT

This study uses graphite, eggshell, and snail shell as friction modifiers in the formulation of bio-hydraulic fluids from palm kernel oil through experimentation and optimization using Response Surface Methodology (RSM). The analyzed samples of graphite, eggshell, and snail shell were characterized using XRD. The bio-hydraulic fluids with graphite, eggshell, and snail shell were optimized using RSM. Sample compositions reveal that graphite contains silicon oxide (30.1%), eggshell contains silicon oxide (10.41%), and snail shell contains silicon oxide (23.4%), indicating that eggshell and snail shell can compete favorably with graphite. FT-IR spectra of the bio-hydraulic fluids with graphite, eggshell, and snail shell reveal functional groups, each having double bond structures and heteroatoms. The optimum conditions for bio-hydraulic fluid viscosity with graphite, eggshell, and snail shell are glycerin/methanol ratio of 20, eggshell dosage of 0.6, and temperature of 60 °C, yielding viscosities of 36.36 cP, 33.61 cP, and 35.21 cP, respectively. The quadratic method describes the relationship between the response (viscosity) and the considered factors adequately. The physicochemical properties of the bio-hydraulic fluids with graphite, eggshell, and snail shell show pour points of -43.9 °C, -40.6 °C, and -39.5 °C, flash points of 253 °C, 245 °C, and 242 °C, viscosities of 36.53 cP, 33.79 cP, and 35.36 cP, and BOD values of 8.51 ppm, 8.12 ppm, and 8.30 ppm, respectively. These values indicate that the bio-hydraulic fluids are suitable for various hydraulic industrial applications. Graphite, eggshell, and snail shell were established as effective friction modifiers in bio-hydraulic fluid formulation.

## KEYWORDS

Bio-hydraulic fluids, Friction modifiers, Eggshell, Snail shell, Optimization, FT-IR, and RSM

## 1. INTRODUCTION

Adding polar molecules to lubricants to lessen light surface contacts (rolling and sliding) that might arise in a given machine design is known as friction modifiers or mild anti-wear agents. They are also known as additives for border lubrication (Noria Corporation, n.d.). The market for friction modifiers was expected to be worth USD 1.15 billion in 2023 and is anticipated to rise at a compound annual growth rate (CAGR) of more than 4.3% from 2024 to 2032 (Global Market Insights, n.d.). The industry comprises additives that affect the frictional characteristics of functional fluids and lubricants to increase their performance in a number of applications, including engineering and automotive vehicles (Global Market Insights, n.d.). By minimizing wear and friction between moving surfaces, these modifiers boost overall operating efficiency, lengthen equipment life, and improve fuel economy. The global market for friction modifiers is rising rapidly due to the increased demand for functional fluids and high-performance lubricants in a range of industries (Lubrizol, 2022).

The United States generates about 150,000 tonnes of eggshell garbage a year, making it a prolific natural waste and a substantial waste product of the food business. The egg industry in Taiwan utilized approximately 50 million egg cartons and wasted more than 120 tonnes of eggshell (Mac, 2001). With fichtelite (42.27%), hanksite (35.07%), and calcite (11.06%),

it offers a lot of potential for a number of purposes. The expected value of the snail goods and delicacies market globally in 2022 was USD 593.4 million (Christian, et al., 2019). Forecasts show that the market will rise at a compound annual growth rate (CAGR) of roughly 10.33% between 2023 and 2032.e41This scenario has led the amount of shell garbage to expand in China, Hong Kong, Japan, Thailand, Taiwan, Nigeria, and Ghana (Deuster and Schmitz, 2021; Esonye, et al., 2019; Marcel, et al., 2020; Houndonougbo, et al., 2012). The two primary components of snail shell are silicon oxide (23.4%) and aragonite (64%). This makes it suited for a number of purposes.

For the aim of performing design of experiments (DOE), Stat-Ease Inc. created the statistical software tool Design-Expert. It enables rigorous parameter design, screening, characterization, optimization, mixed designs, combination designs, and comparison testing. Test matrices are provided from Design-Expert for screening up to 50 variables. Response Surface Methodology (RSM) is a statistical and mathematical approach for studying and improving systems in which multiple variables (inputs) impact the response (output) (Akinpelu, et al., 2021). Widely employed in experimental design, it promotes productivity and generates perfect situations with the least number of testing (Jonah, et al., 2021).

Friction modifiers based on minerals, like metallic oxides, graphite, or molybdenum disulphide, cause major environmental hazards (Global

## Quick Response Code



## Access this article online

Website:  
[www.actachemicamalaysia.com](http://www.actachemicamalaysia.com)

DOI:  
 10.26480/acmy.02.2025.104.110

Market Insights, n.d.).

Sustainable and environmentally friendly friction modifiers made from snail and egg shells are crucial and make good substitutes for creating the viscosity of bio-hydraulic fluids (Lubrizol, 2022). The bio-hydraulic fluid viscosity from graphite, egg, and snail shell is predicted and compared using the experimental Response Surface Methodology (RSM) data generated in this work.

## 2. MATERIALS AND METHODS

### 2.1 Materials

| S/N | Materials/chemicals                  | Function in fluid            | Volume (ml) | Mass (g) |
|-----|--------------------------------------|------------------------------|-------------|----------|
| 1   | Glycerin                             | Recipe base chemical         | 100         | 80.15    |
| 2   | Methanol                             | Formulation solvent          | 4.00        | 2.8      |
| 3   | Graphite or snail shell or egg shell | Friction modifier, anti-wear |             | 0.6      |
| 4   | Diethylene glycol                    | Diluent                      | 1.2         | 1        |
| 5   | Cashew leaf                          | Corrosion inhibitor          |             | 0.3      |
| 6   | polyethylene oxide                   | Anti-foam solvent            | 1.1         | 0.23     |
| 7   | Monoethylene glycol                  | Anti-freezer, coolant        | 1.5         | 1        |

### 2.2 Methods

The pour point of the bio-hydraulic fluid was measured as the lowest temperature at which the fluid flows when cooled under the specified test conditions. A hot specimen was cooled inside a cooling bath to allow the formation of wax crystals. At a temperature slightly above the expected pour point, and for every subsequent X °C decrease, the test jar was removed and tilted to check for surface movement. When the specimen did not flow when tilted, the jar was held horizontally for 5s. When it did not flow, the result was recorded as the pour point temperature.

The flash point of the bio-hydraulic fluid was determined as the temperature at which the vapor over the bio-hydraulic fluid ignited upon exposure to an ignition source. The Cleveland Open Cup (COC) was used to determine the flash point. The sample was contained in an open cup, which was heated, and at intervals, a flame was brought over the surface. The measured flash point varied with the height of the flame above the fluid surface, and at a sufficient height, the measured flash point temperature was recorded.

The viscosity of the bio-hydraulic fluid was measured with a rotational viscometer, which uses a spinning probe immersed in the sample of the bio-hydraulic fluid. Viscosity is a measure of a fluid's resistance to flow, which is caused by the internal resistance to motion. The viscosity was determined by the force needed to rotate the probe at a chosen speed.

The biodegradability of the bio-hydraulic fluid was examined in terms of BOD. The BOD of the bio-hydraulic fluid was determined as the amount of oxygen used by microorganisms as they decompose the organic matter in the sample over a period of time and at a particular temperature. It was carried out in line with the standard method described by (Awoyale et al., 2011). In this test, the standard period and temperature required were five days and 20 °C, respectively. Triplicates of 20 ml of the produced bio-hydraulic fluid, labeled, were mixed with pond water, which contains microorganisms, in incubation bottles, each of which did not allow the passage of light through them. Three other incubation bottles were also filled with 20 ml of mineral bio-hydraulic fluid (controls); 1 ml each of iron (II) chloride, phosphate buffer, calcium chloride, and magnesium sulphate were mixed in 1 liter of distilled water.

The diluted water prepared was added to each of the incubation bottles for about two hours at room temperature, after which the dissolved oxygen was measured using an oxygen meter. The incubation bottles were kept at the same temperature of 20 °C for five (5) days, after which the dissolved oxygen was recorded. The difference in the dissolved oxygen was calculated and recorded. The biodegradability of the bio-hydraulic fluid produced was calculated using Equation (1):

$$BOD = \frac{DO_i - DO_f}{P} * \frac{300}{1000} \quad (1)$$

$$P = \frac{v}{1000} \quad (2)$$

Where BOD (ppm) is the biochemical oxygen demand, DO<sub>i</sub> is the initial dissolve oxygen, DO<sub>f</sub> is the final dissolve oxygen after five days, P is the

The bio-hydraulic fluids stayed formulated using the materials/chemicals in Table 1, in line with the standard method (Eze, 2016). Glycerin obtained from the transesterification reaction of the oil was used as the base substance for the formulation of each bio-hydraulic fluid. Methanol was used as solvent in the blend. The addition of the raw materials was performed in a downward order as shown Tables 1. As the materials have been completely applied into the beaker, it was heated at 60 °C, under stirring condition for 30 minutes.

The egg and snail shell were gotten from Easydon farm and processed.

fraction of the sample, and v= volume of sample (cm<sup>3</sup>).

Fourier transform infrared (FTIR) spectrophotometer was used to identify the fluids functional groups.

After homogenising and fine-grinding the examined sample, the average bulk composition was determined. Then, using the sample preparation block, the powdered sample was compacted in the flat sample holder to produce a smooth, level surface that could be placed on the sample stage in the XRD cabinet. The sample underwent analysis utilising the Theta-Theta settings on the reflection-transmission spinner stage. With a two-theta step of 0.026261 at 8.67 seconds each step, the two-theta starting position was 4 degrees and ended at 75 degrees. The tension was 45VA and the tube current was 40mA. They employed the Gonio Scan and a 5mm Width Mask with a Programmable Divergent Slit. The detector and sample rotated through their respective angles, recording the strength of diffracted X-rays continually. When the material has lattice planes with d-spacings suitable for diffracting X-rays at that value of  $\theta$ , the intensity peaks. Even though each peak has two distinct reflections (K $\alpha$ 1 and K $\alpha$ 2), the peak positions overlap at tiny values of 2 $\theta$ , with K $\alpha$ 2 showing up as a hump on the side of K $\alpha$ 1. Higher  $\theta$  values result in more separation. These conjoined peaks are usually handled as a single entity. The centre of the peak at 80% peak height is often used to calculate the 2 $\lambda$  position of the diffraction peak. The results showed X-ray counts (intensity) and peak locations at 2 $\theta$  (Ezeugo and Ikebudu, 2019).

### 2.3 Design of experiment and optimization of the bio-hydraulic fluid Viscosities

Using RSM, Interactive effects of process variables of glycerin/methanol ratio (10 - 30), graphite or egg or snail shells dosage (0.2 - 1.0), temperature (50 °C - 70 °C) and time (20 min. - 40 min.) on the viscosity of each bio-hydraulic fluid were determined. The experiment was designed using Design Expert software version 11. The process involves analysis of variance, mathematical modelling, and validation of optimum results (Fan, et al., 2011).

## 3. RESULTS AND DISCUSSION

### 3.1 Results of XRD characterization of the graphite, egg and snail shells

Results of XRD characterization of the graphite, egg and snail shells are displayed in Figures 1, 2 and 3 respectively. As shown in Figure 1, graphite contains 58.5% calcite. Other constituents of the graphite include silicon oxide (30.1%), urea, hanksite, periclase and aluminium phosphate. Various peaks of the graphite also revealed that calcite and silicon oxide are the major mineralogical constituents of graphite. In Figure 2, fichtelite (42.27%), hanksite (35.07%) and calcite (11.06%) were revealed as the predominant constituents of egg shell. Other constituents include aluminium and epsomite, which appeared in traces. Similarly, mineralogical constituents of the snail as shown in Figures 3 include aragonite (64%) and silicon oxide (23.4%) as the major constituents of snail shell. Other revealed constituents of the snail shell were periclase, refikite, aluminium and hanksite.

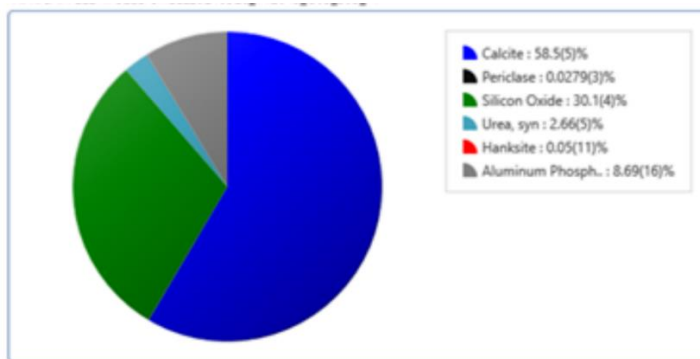


Figure 1: Pie chart of the XRD result of graphite

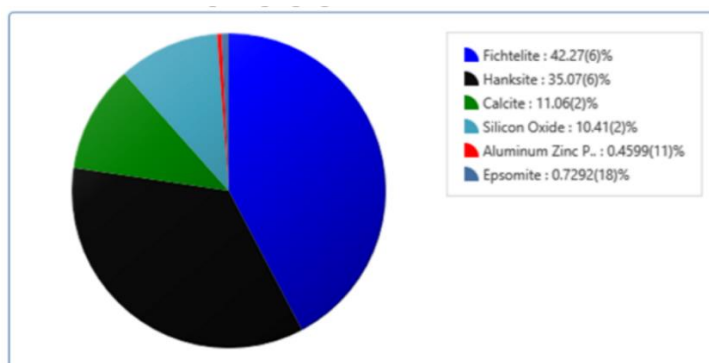


Figure 2: Pie chart of the XRD result of egg shell

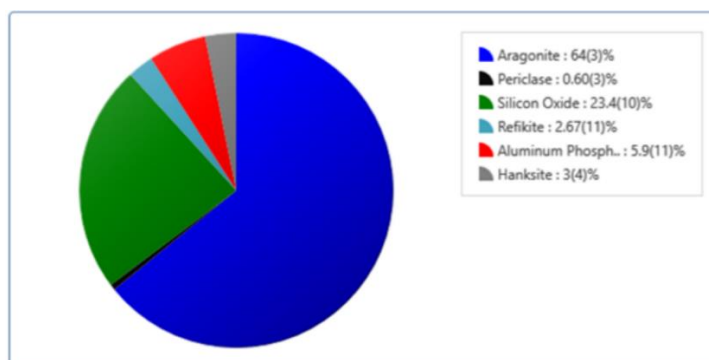


Figure 3: Pie chart of the XRD result of snail shell

### 3.2 Physiochemical analysis and FTIR characterization and of the bio-hydraulic fluids.

Figures 4 – 6 show the spectra of the bio-hydraulic fluid made with graphite, egg and snail shells as friction modifiers. Each spectrum displays the relationship between wave number and transmittance, with different peaks signifying the functional groups. Each of them has double bond structures and heteroatoms. The bio-hydraulic fluids are suitable for lubricating and allied functions (Eevera, et al., 200; Esonye, et al., 2019;

Onukwuli and Omotioma, 2016). The physiochemical analysis of the bio-hydraulic fluids using graphite, egg and snail shell gave Pour point -43.9°C, -40.6°C and -39.5°C, Flash point 253°C, 245°C and 242°C, Viscosity 36.53cP, 33.79cP and 35.36cP and BOD of 8.51ppm, 8.12ppm and 8.30ppm respectively. The result falls within the range of the mineral base hydraulic fluid “Mineral base hydraulic fluid” Pour point > -20°C, Flash point 180 to -350°C, viscosity >25cP and Biochemical oxygen demand >15ppm. These properties show that the bio-hydraulic fluid is suitable for various hydraulic industrial applications.



Sample ID: H  
 Sample Scans: 32  
 Background Scans: 16  
 Resolution: 8  
 System Status: Good  
 File Location: C:\Program Files\Agilent\MicroLab PC\Results\H\_9-4-2024\T7-35-31 PM.a2r

Method Name: Transmittance  
 User: Admin  
 Date/Time: 2024-09-04T19:35:31.173-07:00  
 Range: 4000 - 650  
 Apodization: Happ-Genzel

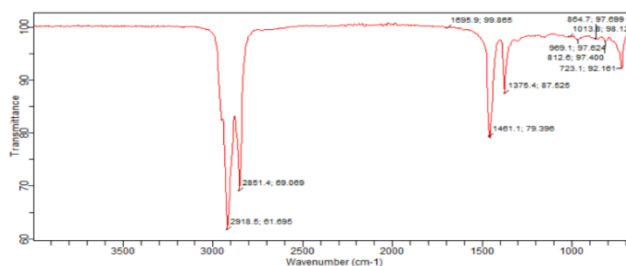


Figure 4: Spectrum of the bio-hydraulic fluid using graphite as friction modifier

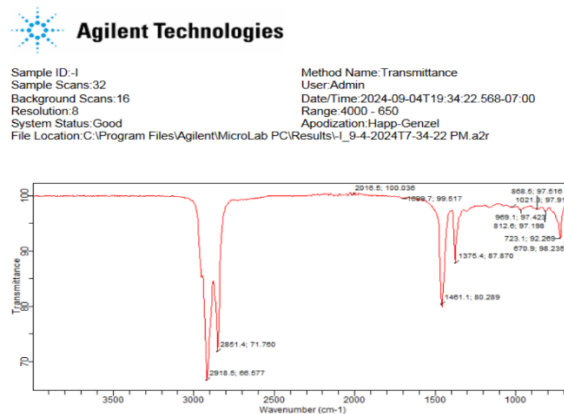


Figure 5: Spectrum of the bio-hydraulic fluid using egg shell as friction modifier

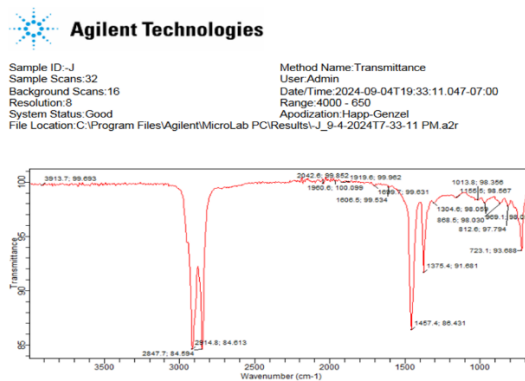


Figure 6: Spectrum of the bio-hydraulic fluid using snail shell as friction modifier

3.2 Model fit summary and Analysis of variance (ANOVA)

ANOVA data were analyzed to determine the quadratic model of the viscosities of the bio-hydraulic fluid formulated with graphite, egg shell, and snail shell and its optimal reaction conditions. Equations 3 – 5 present a quadratic equation model of the viscosities of the bio-hydraulic fluid in terms of coded factors. This was done in order to optimise the interactive effects of the variables on the viscosity of the bio-hydraulic fluid.

Model in terms of coded factors of bio-hydraulic fluid using graphite as friction modifier

$$\text{Viscosity} = +36.36 + 1.28A + 1.06B - 0.2667C + 0.6400D + 0.4415AB + 0.4331AC + 0.3406AD - 0.1306BC + 0.3569BD - 0.0269CD - 1.86A^2 - 1.34B^2 - 0.1245C^2 - 1.04D^2 \quad (3)$$

Model in terms of coded factors of bio-hydraulic fluid using egg shell as friction modifier

$$\text{Viscosity} = +33.61 + 1.27A + 1.06B - 0.2594C + 0.6394D + 0.4475AB + 0.4300AC + 0.3488AD - 0.1387BC + 0.3425BD - 0.0425CD - 1.86A^2 - 1.33B^2 - 0.1339C^2 - 1.05D^2 \quad (4)$$

Model in terms of coded factors of bio-hydraulic fluid using snail shell as friction modifier

$$\text{Viscosity} = +35.21 + 1.27A + 1.06B - 0.2789C + 0.6422D + 0.4456AB + 0.4294AC + 0.3481AD - 0.1369BC + 0.3469BD - 0.0394CD - 1.86A^2 - 1.33B^2 - 0.0811C^2 - 1.05D^2 \quad (5)$$

Table 2 shows the result of RSM for viscosities of the bio-hydraulic fluid formulations. The Table revealed how the process factors interacted to affect the viscosity. It forms the basis for the optimization process (Alamu, et al., 2007; Onukwuli and Omotioma, 2016; Omotioma, et al., 2021). The results were analysed by multiple regression analysis in table 3.

| Table 2: Result of the RSM for viscosity of bio-hydraulic fluid using graphite as friction modifier |     |                          |                    |           |            |               |
|---|-----|--------------------------|--------------------|-----------|------------|---------------|
| Std   | ERN | Glycerin/ methanol ratio | Graphite dosage, g | Temp., °C | Time, min. | Viscosity, cP |
| 14  | 1   | 30                       | 0.2                | 70        | 40         | 32.71         |
| 24  | 2   | 20                       | 0.6                | 60        | 40         | 35.98         |
| 3   | 3   | 10                       | 1                  | 50        | 20         | 31.75         |
| 5   | 4   | 10                       | 0.2                | 70        | 20         | 30            |
| 8   | 5   | 30                       | 1                  | 70        | 20         | 33.62         |
| 6   | 6   | 30                       | 0.2                | 70        | 20         | 31.21         |
| 9   | 7   | 10                       | 0.2                | 50        | 40         | 30.83         |
| 15  | 8   | 10                       | 1                  | 70        | 40         | 31.27         |
| 1   | 9   | 10                       | 0.2                | 50        | 20         | 30.63         |
| 2   | 10  | 30                       | 0.2                | 50        | 20         | 30.92         |
| 21  | 11  | 20                       | 0.6                | 50        | 30         | 36.01         |
| 16  | 12  | 30                       | 1                  | 70        | 40         | 35.99         |
| 25  | 13  | 20                       | 0.6                | 60        | 30         | 36.53         |
| 17  | 14  | 10                       | 0.6                | 60        | 30         | 32.68         |

| Table 2 (cont): Result of the RSM for viscosity of bio-hydraulic fluid using graphite as friction modifier |    |    |     |    |    |       |
|--|----|----|-----|----|----|-------|
| 19   | 15 | 20 | 0.2 | 60 | 30 | 33.7  |
| 28   | 16 | 20 | 0.6 | 60 | 30 | 36.53 |
| 11   | 17 | 10 | 1   | 50 | 40 | 32.91 |
| 20   | 18 | 20 | 1   | 60 | 30 | 35.99 |
| 10   | 19 | 30 | 0.2 | 50 | 40 | 32.2  |
| 13   | 20 | 10 | 0.2 | 70 | 40 | 29.25 |
| 26   | 21 | 20 | 0.6 | 60 | 30 | 36.53 |
| 12   | 22 | 30 | 1   | 50 | 40 | 35.95 |
| 29   | 23 | 20 | 0.6 | 60 | 30 | 36.53 |
| 27   | 24 | 20 | 0.6 | 60 | 30 | 36.53 |
| 4  | 25 | 30 | 1   | 50 | 20 | 33.45 |
| 30   | 26 | 20 | 0.6 | 60 | 30 | 36.53 |
| 18   | 27 | 30 | 0.6 | 60 | 30 | 36.01 |
| 22   | 28 | 20 | 0.6 | 70 | 30 | 36.12 |
| 7  | 29 | 10 | 1   | 70 | 20 | 29.68 |
| 23   | 30 | 20 | 0.6 | 60 | 20 | 34.31 |

It is necessary to estimate the analysis of variance on each model coefficient test for lack-of-fit in order to guarantee a comprehensive model fit. A model's inability to accurately depict data that cannot be provided by random error is measured by its lack-of-fit (Tabrizi and Nassaj, 2011). The F-value or P-value, also referred to as a probability of error value or "prob > F" value, is typically used to determine the relevant process factors (Tabrizi and Nassaj, 2011). The associated coefficient is more significant when the F-value is larger and the "prob > F" value is less (Tabrizi and Nassaj, 2011).

Table 3 provide a summary of the second-order response surface model findings for the friction modifiers in the form of an ANOVA. The model's F-value is 128.83, 117.58, and 114.21, as shown in the tables, and its

related P-value (prob > F) is very tiny, at less than 0.0001, suggesting that the model is highly significant. We use the P-values as a tool to make sure that each co-efficient is important. An F-value this enormous could only be the result of noise in 0.01% of cases. Model terms are considered significant when the P-value is less than 0.0500. A, B, C, D, AB, AC, AD, BD, A2, B2, and D2 are important model terms in this instance. Adeq Precision evaluates the signal to noise ratio, and the Predicted R2 of 0.9841, 0.9521, and 0.9590 are in acceptable agreement with the Adjusted R2 of 0.9841, 0.9825, and 0.9857, respectively; that is, the difference is less than 0.2. More over four is the ideal ratio. The ratios of 31.50, 30.03, and 33.642 show that the signal is sufficient. Regarding the link between the response variable and the independent process variables, this model offers a great explanation (Ezeugo, 2019; Ezeugo, et al., 2019).

| Table 3: ANOVA for Quadratic model of Viscosity of bio-hydraulic fluid using graphite as friction modifier |                |    |             |                          |          |             |
|--|----------------|----|-------------|--------------------------|----------|-------------|
| Source   | Sum of Squares | df | Mean Square | F-value                  | p-value  |             |
| Model  | 180.06         | 14 | 12.86       | 128.83                   | < 0.0001 | significant |
| A-Glycerin/ methanol ratio   | 29.54          | 1  | 29.54       | 295.91                   | < 0.0001 |             |
| B-Graphite dosage  | 20.39          | 1  | 20.39       | 204.28                   | < 0.0001 |             |
| C-Temperature  | 1.28           | 1  | 1.28        | 12.82                    | 0.0027   |             |
| D-Time   | 7.37           | 1  | 7.37        | 73.85                    | < 0.0001 |             |
| AB   | 3.12           | 1  | 3.12        | 31.29                    | < 0.0001 |             |
| AC   | 3.00           | 1  | 3.00        | 30.07                    | < 0.0001 |             |
| AD   | 1.86           | 1  | 1.86        | 18.59                    | 0.0006   |             |
| BC   | 0.2730         | 1  | 0.2730      | 2.73                     | 0.1190   |             |
| BD   | 1.82           | 1  | 1.82        | 18.19                    | 0.0007   |             |
| CD   | 0.0116         | 1  | 0.0116      | 0.1158                   | 0.7384   |             |
| A <sup>2</sup>   | 8.81           | 1  | 8.81        | 88.29                    | < 0.0001 |             |
| B <sup>2</sup>   | 4.68           | 1  | 4.68        | 46.91                    | < 0.0001 |             |
| C <sup>2</sup>   | 0.0401         | 1  | 0.0401      | 0.4021                   | 0.5356   |             |
| D <sup>2</sup>   | 2.83           | 1  | 2.83        | 28.31                    | < 0.0001 |             |
| Residual   | 1.50           | 15 | 0.0998      |                          |          |             |
| Lack of Fit  | 1.50           | 10 | 0.1498      |                          |          |             |
| Pure Error   | 0.0000         | 5  | 0.0000      |                          |          |             |
| Cor Total  | 181.56         | 29 |             |                          |          |             |
| Std. Dev.  | 0.3160         |    |             | R <sup>2</sup>           |          | 0.9918      |
| Mean   | 33.74          |    |             | Adjusted R <sup>2</sup>  |          | 0.9841      |
| C.V. %   | 0.9363         |    |             | Predicted R <sup>2</sup> |          | 0.9580      |
|  |                |    |             | Adeq Precision           |          | 31.4978     |

### 3.2.1 3-D plots of the viscosity of the bio-hydraulic fluids and Validation of RSM model.

Three-dimensional plots of viscosity of the bio-hydraulic fluid are shown in figure 7. It demonstrate how the process factors interact to affect the viscosity of the fluids reveal parabolic graph. It then verified that there is

a quadratic link between the response (viscosity) and the factors taken into consideration in the formulation of the fluid (Esonye, et al., 2019; Minodora, et al., 2010). Table 4 shows the interactive effects of the process

variables and validation of RSM data of dropping of the bio-hydraulic fluids. This reveal how close the optimum (predicted) viscosity is to the experimental viscosity of the bio-hydraulic fluid. The determined percentage deviation is less than 5%. The RSM results were validated.

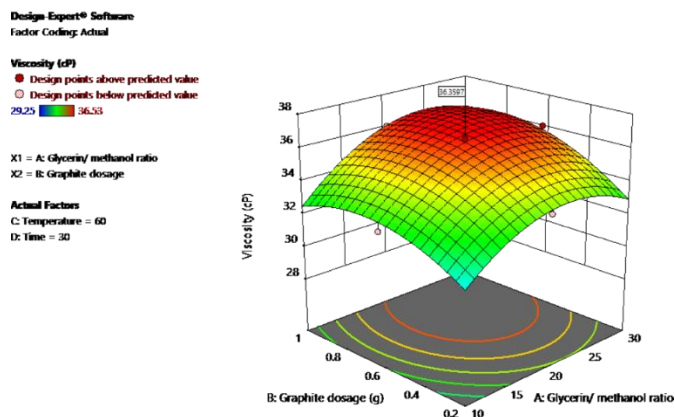


Figure 7: Viscosity of bio-hydraulic fluid

| Table 4: The interactive effects of the process variables on viscosity and validation of RSM data of dropping point of the bio-hydraulic fluids |                          |           |           |            |                          |                     |                          |
|---|--------------------------|-----------|-----------|------------|--------------------------|---------------------|--------------------------|
| Bio-hydraulic type  | Glycerin/ methanol ratio | Dosage, g | Temp., °C | Time, min. | Predicted viscosity (cP) | Exp. viscosity (cP) | Percentage deviation (%) |
| Bio-hydraulic fluid with graphite   | 20                       | 0.6       | 60        | 30         | 36.36                    | 36.13               | 0.64                     |
| Bio-hydraulic fluid with egg  | 20                       | 0.6       | 60        | 30         | 33.61                    | 32.92               | 2.10                     |
| Bio-hydraulic fluid with snail  | 20                       | 0.6       | 60        | 30         | 35.21                    | 35.06               | 0.43                     |

Dosage referred to the graphite dosage, egg dosage and snail dosage in the respective cases

### 3.2.2 Diagnostic reports of the RSM results of the bio-hydraulic fluids viscosity

Figures 8 shows the Predicted verses Actual of the viscosity and Residuals verses run of the viscosity of bio-hydraulic fluid. Figure 9 reveals residuals scattering randomly across the predictions. The experimentally measured values of viscosity. Y-axis (Predicted): The viscosity values predicted by

the RSM model, based on the fitted polynomial equation. The consistent alignment across the range shows that the model performs well for both low and high viscosity values. Most data points clustered around the line of best fit, indicating a good fit between the predicted and actual values (Chitra, et al., 2005; Dumancas, et al., 2016). This suggests that the RSM model reliably predict the viscosity of the bio-hydraulic fluid based on the considered factors.

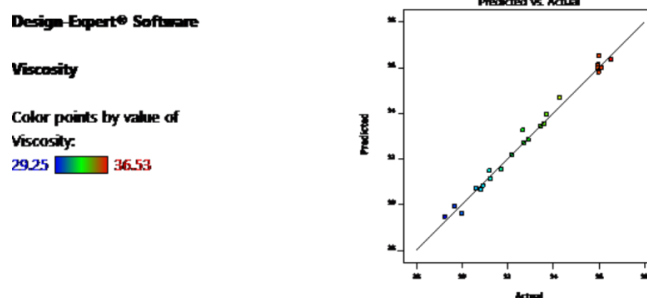


Figure 8: The predicted verses Actual viscosity of bio-hydraulic fluid

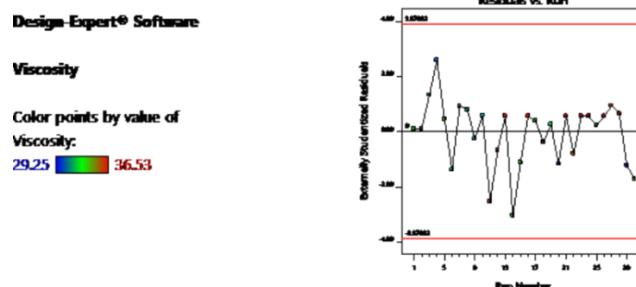


Figure 9: Residuals verses run of the viscosity of the viscosity of bio-hydraulic fluid

### 3.3 Physicochemical Properties of the Bio-Hydraulic Fluids

The physicochemical properties of the bio-hydraulic fluid produced using graphite, eggshell, and snail shell based on pour point (-43.9, -40.6, -39.5°C), flash point (253, 245, 242°C), viscosity (36.53, 33.79, 35.36cP), and biochemical oxygen demand (8.51, 8.12, 8.30ppm). This values are within ASTM standards for biohydraulic and mineral based fluids

properties.

## 4. CONCLUSIONS

Eggshell and snail shell were established as friction modifiers in the formulation of bio-hydraulic fluids. The XRD results indicated that graphite, eggshell, and snail shell were suitable friction modifiers and anti-

wear agents for hydraulic fluids. The eggshell and snail shell exhibited mineralogical properties. The optimum conditions for bio-hydraulic fluid viscosity with graphite, eggshell, and snail shell as friction modifiers were a glycerin/methanol ratio of 20, an eggshell dosage of 0.6, and a temperature of 60 °C, yielding optimum viscosities of 36.36 cP, 33.61 cP, and 35.21 cP, respectively.

ANOVA and the quadratic model provided a clear explanation of how the process variables interacted. The model was also examined and validated through three-dimensional plots of the bio-hydraulic fluid's viscosity, showing a parabolic curve. The comparative evaluation of the bio-hydraulic fluids revealed that the bio-hydraulic fluid formulated with snail shell had higher viscosity than that with eggshell. This also indicates that eggshell and snail shell can compete favorably as friction modifiers and are suitable alternatives to graphite. The bio-hydraulic fluids are suitable for various hydraulic applications.

## ACKNOWLEDGEMENTS

The authors acknowledge our father, Benneth Tochukwu Ifediorah, for his encouragement and motivation throughout this research work. We acknowledge the Chemical Engineering Laboratory, Chemical Engineering Department, Chukwuemeka Odumegwu Ojukwu University, Anambra State, Nigeria, for its support.

## Credit Authorship Contribution Statement

Ifediorah Ezekiel: Conceptualization, Methodology, Software Data curation, Writing, Original draft preparation. Visualization, Investigation. Software and Validation.

Ezeugo Joseph: Supervision, Reviewing and Editing.

## Declaration of competing interest

The authors declare that they have no known competing financial interests or personal relationships that could have appeared to influence the work reported in this paper.

## REFERENCES

Akinpelu K.B., Okechukwu, D.O., Eluno E.E., 2021. Optimizing process parameters of palm oil bleaching on locally prepared animal bone based activated carbon using response surface methodology. *Environmental Quality Management*. 30(5), Pp. 224-234. <http://dx.doi.org/10.1002/tqem.21729>.

Alamu, O.J., Waheed, M.A., Jekayinfa, S.O., 2007. Alkali-catalysed laboratory production and testing of biodiesel fuel from Nigerian palm kernel oil. *Agricultural Engineering International: The CIGR Ejournal*, EE07 009, Pp. 1-11.

Chitra, P., Venkatachalam, P., Sampathrajan, A., 2005. Optimization of experimental conditions for biodiesel production from alkali-catalyzed transesterification of *Jatropha curcas* oil. *Energy for Sustainable Development* 9 (3), Pp. 13-18.

Christian, K.M., Annick, E.N., Siri, B.N., Kingsley, E., 2019. Socio-economic perception of snail meat consumption in Fako Division, South-West Region Cameroon. *International Journal of Livestock Production* 10, Pp. 143-151. <https://doi.org/10.5897/IJLP2018.0559>.

Deuster, S., Schmitz, K., 2021. Bio-based hydraulic fluids and the influence of hydraulic oil viscosity on the efficiency of mobile machinery. *Sustainability* 13, Pp. 570. <https://doi.org/10.3390/su13020570>.

Dumancas, G., Patel, V., Viswanath, L., Maples, R., Subong, B.J., 2016. Castor oil: Properties, uses, and optimization of processing parameters in commercial production. *Lipid Insights*, Pp. 1-12. <https://doi.org/10.4137/LPI.S40233>.

Eevera, T., Rajendran, K., Saradha, S., 2009. Biodiesel production process optimization and characterization to assess the suitability of the product for varied environmental conditions. *Renewable Energy* 34, Pp. 762-765. <https://doi.org/10.1016/j.renene.2008.04.006>.

Esonye, C., Onukwuli, O.D., Ofoefule, A.U., 2019. Optimization of methyl ester production from *Prunus amygdalus* seed oil using response surface methodology and artificial neural networks. *Renewable Energy* 130, Pp. 61-72. <https://doi.org/10.1016/j.renene.2018.06.036>.

Eze, C.C., 2016. Formulation and production of bio-hydraulic fluid as an alternative to mineral fluids for automobiles. *American Journal of Engineering Research (AJER)* 5 (10), Pp. 147-151.

Ezeugo, J.N.O., 2019. A design and an optimization of eco-friendly extract for inhibition of mild steel corrosion in sulphuric acid media. *Journal Chemical Technology and Metallurgy*, 54 (4), Pp. 810-825.—JCTM

Ezeugo, J.O. and Ikebundu K.O., 2019. Evaluation of plant extract as anti-corrosion for zinc in 1.0 M HCL. Using response surface methodology. *Int. J. Advanced Engineering & Techn.*, 3 (1, Pp. 01 - 09--IJAET.

Ezeugo, J.O., Ezechukwu, V.C., Nwaeto, L.O., Onukwuli, O.D., Ikebundu, K.O., 2019. Optimization of chrysophyllum albidum leaf extract as corrosion inhibitor for aluminium in 0.5 M H<sub>2</sub>SO<sub>4</sub>. *World Scientific News*. 125, Pp. 32 - 50. WSN - AISJ (b)

Fan, X., Wang, X., Chen, F., 2011. Biodiesel production from crude cottonseed oil: An optimization process using response surface methodology. *The Open Fuels and Energy Science Journal* 4, Pp. 1-8. <https://doi.org/10.2174/1876973X01104010001>.

Ghosh, S., Jung, C., Rochow, V.B.M., 2017. Snail as mini-livestock: Nutritional potential of farmed *Pomacea canaliculata* (Ampullariidae). *Agriculture and Natural Resources* 51, Pp. 504-511. <https://doi.org/10.1016/j.anres.2017.10.003>.

Global Market Insights, n.d. Friction modifiers market - Type of modifiers (organic friction modifiers, organomolybdenum friction modifiers, polymer friction modifiers), by compound type (organic, inorganic), by applications and forecast, 2024-2032. Available at: <https://www.gminsights.com/industry-analysis/friction-modifiers-market> (Accessed 21 December 2024).

Houndonougbo, M.F., Chwalibog, A., Chrysostome, C.A.A.M., 2012. Effect of processing on feed quality and bio-economic performances of broiler chickens in Benin. *International Journal of Applied Poultry Research* 1, Pp. 47-54.

Jonah, C. U., Stanley, O., Chidozie C.W., Okechukwu, D.O., 2021. Computational modeling and multi-objective optimization of engine performance of biodiesel made with castor oil. Elsevier. DOI: 10.1016/j.heliyon.2021.e06516.

Leung, D.Y.C., Guo, Y., 2006. Transesterification of neat and used frying oil: Optimization for biodiesel production. *Fuel Processing Technology* 87 (10), Pp. 883-890. <https://doi.org/10.1016/j.fuproc.2006.06.003>.

Lubrizol, 2022. What additive components are in your hydraulic fluid? Available at: <https://360.lubrizol.com/2022/What-Additive-Components-Are-in-Your-Hydraulic-Fluid> (Accessed 21 December 2024).

Mac, N.J.H., 2001. Method and apparatus for separating a protein membrane and shell material in waste eggshell. U.S. Patent No. 6,176,376.

Marcel, K.N., Rosemonde, Y.E.S., Patricia, K.A., Alexandre, Z.B.F.G., Ambroise, A.N., Ernest, A.K., 2020. Evaluation of the nutritional potential of snail (*Achatina* spp) meat in rat. *European Scientific Journal* 16, Pp. 111-121. <https://doi.org/10.19044/esj.2020.v16n6p111>.

Minodora, L., Luminița, T., Marin, M., Teodora, S., 2010. Optimization of biodiesel production by transesterification of vegetable oils using lipases. *Romanian Biotechnological Letters* 15 (5), Pp. 5618-5630.

Noria Corporation, n.d. Understanding biohydraulic fluids: Properties and applications. Available at: <https://www.noria.com> (Accessed 21 December 2024).

Omotioma, M., Okezue, C.F., Obiora-Okafor, I.A., 2021. Bamboo (*Bambusoideae*) leaf on the detoxification of cassava wastewater for potential biogas production. *Journal of Water Chemistry and Technology* 43 (1), Pp. 40-45. <https://doi.org/10.3103/S1063455X21010066>.

Onukwuli, O.D., Omotioma, M., 2016. Optimization of the inhibition efficiency of mango extract as corrosion inhibitor of mild steel in 1.0 M H<sub>2</sub>SO<sub>4</sub> using response surface methodology. *Journal of Chemical Technology and Metallurgy* 51 (3), Pp. 302-314.

Tabrizi, S.A.H., Nassaj, E.T., 2011. Modelling and optimization of densification of nanocrystalline Al<sub>2</sub>O<sub>3</sub> powder prepared by a sol-gel method using response surface methodology. *Journal of Sol-Gel Science and Technology* 57, Pp. 212-220. <https://doi.org/10.1007/s10971-010-2346-6>.